Swelling, Elasticity, and Spatial Inhomogeneity of Poly(*N*-isopropylacrylamide)/Clay Nanocomposite Hydrogels

Jingjing Nie, Binyang Du, and Wilhelm Oppermann*

Institute of Physical Chemistry, Clausthal University of Technology, Arnold-Sommerfeld Str. 4, 38678 Clausthal-Zellerfeld, Germany

Received March 21, 2005; Revised Manuscript Received May 4, 2005

ABSTRACT: Static light scattering measurements reveal two levels of organization, i.e., two static correlation lengths, in poly(*N*-isopropylacrylamide)/clay nanocomposite hydrogels prepared by polymerizing the monomer in an aqueous suspension of uniformly dispersed exfoliated clay particles. One characteristic correlation length is in the range of 200−250 nm irrespective of the preparation conditions. It is assumed to arise from a kinetically controlled rearrangement of the clay particles during the formation of the gels. The other correlation length of several tens of nanometers is in the same order of magnitude as that observed in chemically cross-linked gels and shows a similar dependence on the preparation conditions. The shear modulus of the gels rises with increasing the clay concentration and the monomer concentration. The results infer that clay particles act as multifunctional cross-links with an average effective functionality around 50. Measurements of the equilibrium swelling ratio are in agreement with this view.

Introduction

The properties of thermosensitive poly(*N*-isopropylacrylamide) (PNIPA) hydrogels have been intensively studied because of many important potential applications.[1−4] Moreover, there is a fundamental scientific interest in understanding the structure−property relationships in such systems, in particular the formation of heterogeneous microstructures in cross-linked systems and their influence on elasticity, swelling behavior, and thermoreversible phase change.[5−11] Usually, the PNIPA hydrogels are prepared by free-radical copolymerization of the monomer (NIPA) and a chemical cross-linker such as *N,N′*-methylenebis(acrylamide) (BIS). It was shown recently that the polymerization of NIPA in the presence of inorganic clay particles results in hydrogels with improved mechanical and swelling−deswelling properties.[12−17] This is thought to be due to strong interactions at the clay−polymer interface and the combination of polymer and inorganic components within a single material on a nanoscale level. Such nanocomposite gels are attractive for a wide range of applications.

Several kinds of inorganic clay particles have been introduced into PNIPA gel systems with or without additional use of chemical cross-linkers. These comprise e.g. Na-montmorillonite,[12,13] quaternary alkylammonium-exchanged montmorillonite,[14] and synthetic hectorite "Laponite XLG".[15,16] Haraguchi et al.[15,16] reported that Laponite is particularly attractive because the exfoliated clay particles are uniformly dispersed and act as multifunctional cross-links. The incorporation of this clay markedly improves not only the mechanical and swelling−deswelling properties but also the spatial homogeneity of the nanocomposite gels. These authors used optical transparency to get an estimate of spatial homogeneity. They also proposed a structural model to account for the improvement of physical properties.

* To whom correspondence should be addressed. E-mail: wilhelm.oppermann@tu-clausthal.de.

Recently, Shibayama et al.[18] investigated the structure and dynamics of PNIPA−Laponite XLG hydrogels by small-angle neutron scattering and dynamic light scattering. Their results show that the mesh size of such hydrogels and the inhomogeneities are governed by the concentration of clay, while the chain dynamics are similar to those of conventional, chemically cross-linked PNIPA gels. With regard to the inhomogeneities, they argued that the PNIPA chains are anchored to the clay particles in such a way that there is an excess polymer density close to the surface of the platelets.

To broaden our knowledge on the key factors that control the microstructure and the spatial inhomogeneity of such systems and to compare their behavior with that of conventional hydrogels, we performed a systematic study on PNIPA/Laponite RDS nanocomposite gels prepared with different clay content, different monomer concentration, and different preparation temperature. The gels were made without any chemical cross-linker. In this paper, we present and discuss the results of modulus and swelling measurements as well as those of static light scattering experiments. The static light scattering results show that the microscopic structure of nanocomposite hydrogels differs markedly from what was previously found with chemically cross-linked PNIPA.[11]

Experimental Section

Sample Preparation. *N*-Isopropylacrylamide (NIPA, ACROS), potassium peroxodisulfate ($K_2S_2O_8$, Sigma), and *N,N,N′,N′*-tetramethylethylenediamine (TEMED, Sigma) were used as received. The synthetic hectorite clay, Laponite RDS ($Na^+_{0.7}[(Si_8Mg_{5.5}Li_{0.3})O_{20}(OH)_4]^{0.7-}$, modified with pyrophosphate ions ($P_2O_7^{4-}$)), was kindly provided by Rockwood Ltd. Suspensions of Laponite RDS were newly prepared right before use by dispersing the white powder at the preset concentrations in deionized water under vigorous stirring for at least 1 h. The stability of the clay dispersion was checked by light scattering measurements. When left standing at room temperature for 2 days, the scattering intensities did change less than 10%. Similar stability was observed when NIPA monomer was added.

10.1021/ma050589s CCC: $30.25 © 2005 American Chemical Society
Published on Web 05/28/2005

Table 1. Preparation Conditions and Some Relevant Results

C_{NIPA} (mM)	C_{RDS} (g/mL)	T_{prep} (°C)	ϕ_0 (%)	G_0 (Pa)	ν_{eff} (mol/m^3)	f_{eff}	N	q	N_q
646	*0.01*	25.0	4.93	691	5.66	95	1740	110	870
646	*0.02*	25.0	5.67	799	5.68	55	1730	125	940
646	*0.03*	25.0	6.04	958	6.40	44	1540	145	1130
646	*0.04*	25.0	6.07	1350	8.97	46	1100	144	1110
646	*0.05*	25.0	6.43	1690	10.6	46	930	144	1050
465	0.03	25.0	4.35	643	5.97	29	1650	141	1470
549	0.03	25.0	5.13	780	6.13	36	1610	138	1210
600	0.03	25.0	5.16	872	6.27	40	1570	144	1190
646	0.03	25.0	6.04	958	6.40	44	1540	145	1130
743	0.03	25.0	6.94	1090	6.34	50	1550	138	910
646	*0.05*	*20.0*	6.43	1700	10.9	48	906	133	920
646	*0.05*	*22.5*	6.43	1690	10.7	47	920	135	950
646	*0.05*	*25.0*	6.43	1720	10.8	47	910	144	1050
646	*0.05*	*27.5*	6.43	1660	10.3	45	950	152	1150
646	*0.03*	*20.0*	6.04	916	6.23	43	1580	116	790
646	*0.03*	*25.0*	6.04	1000	6.68	46	1470	145	1130
646	*0.03*	*30.0*	6.04	959	6.30	43	1560	149	1180

PNIPA hydrogels were prepared by free-radical cross-linking copolymerization of NIPA and Laponite RDS mixed in an aqueous solution in the presence of 1.6 mM $K_2S_2O_8$ initiator and 5.4 mM TEMED accelerator. In detail, NIPA solution was first added from a stock solution into a Laponite RDS suspension in a small beaker under stirring; a stock solution of $K_2S_2O_8$ initiator was then added under stirring; at the end, TEMED accelerator was added by using a microsyringe. The solution was then filtered into light scattering vials having 8 mm inner diameter shortly after the addition of TEMED. Nylon membrane filters of 0.2 μm pore size were used. Corresponding solutions of linear polymer were obtained by free-radical polymerization under identical conditions in the absence of Laponite RDS. For all of the solutions, deionized water was used. Temperature control was achieved by a water bath. To obtain gels for the mechanical measurements, they were prepared in similar vials with two open ends to enable easier removal of the gels. Details about the conditions applied to synthesize the gels are listed in Table 1**.** Several series of gels were prepared where the monomer concentration, the clay concentration, or the preparation temperature was varied systematically, keeping the other parameters fixed.

Mechanical Measurements. Uniaxial compression measurements were performed on the gels at room temperature. The gels were cut into cylindrical samples of about 16 mm length. The stress−strain isotherms were measured by using an apparatus described elsewhere.[19] The shear modulus of the gel, G_0, was determined by

$$\sigma = G_0(\lambda - \lambda^{-2}) \tag{1}$$

where σ is the stress applied onto the gel and λ is the deformation ratio (length at deformation/initial length).

Swelling Ratio Measurements. The hydrogels with 8 mm diameter were cut into samples of about 16 mm length and immersed into a large excess of water at room temperature for about 1 month. The water was frequently replaced. On reaching swelling equilibrium, the gels were gently wiped with filter paper and weighed to give W_s. Gels were then dried in an oven at 50 °C for about 7 days. On reaching constant weights, the gels were weighed to give W_d. The mass ratio of polymer and clay in the dried samples was determined by thermogravimetry making use of the chemical decomposition of the polymer around 400 °C. Comparison of the actual mass ratio m_{poly}/m_{clay} with the ratio m_{NIPA}/m_{clay} used for synthesis gave the sol fraction, which was less than 12% for all samples except the one made with only 0.01 g/mL of clay. The equilibrium swelling ratio, q, being related to the unextractable polymer only is given by

$$q = (1 + m_{clay}/m_{poly})W_s/W_d \tag{2}$$

Static Light Scattering Measurements. Static light scattering measurements were performed at 25 °C in the angular range 30°−140° using a goniometer SLS-2 equipped with a He−Ne laser (λ = 632.8 nm). The absolute intensity was calibrated against a toluene standard. To obtain correct spatial averaging, six measurements at different positions achieved by a 60° rotation of the vial between successive measurements were made.

Results and Discussion

The PNIPA/Laponite RDS nanocomposite hydrogels obtained in the present study are transparent and show large and reversible elongation and bending properties similar to what had been reported by Haraguchi et al.[15,16] They exhibit large, but finite, swelling when placed in an excess of water. This behavior is a strong proof of the fact that the gels are permanently cross-linked, although we do not know the detailed nature of the binding of PNIPA to the clay particles, i.e., whether it is covalent tethering or (irreversible) chain adsorption. To gain insight into the properties of the networks on a macroscopic and microscopic scale, the elasticity, the swelling behavior, and the spatial homogeneities were systematically investigated as a function of the preparation conditions.

Elasticity. For a network of Gaussian chains, the effective network density ν_{eff} (number of active network chains per volume of dry network) is related to the shear modulus G_0 measured in the state of gel preparation by[20,21]

$$G_0 = A\nu_{eff}RT\phi_0 \tag{3}$$

In eq 3, R is the gas constant, T the absolute temperature, and ϕ_0 the polymer volume fraction at sample preparation. The structure factor A equals 1 for an affine network and $1 - 2/f$ for a phantom network, where f is the functionality of the cross-links. We will prove below that the clay particles act as multifunctional cross-links, i.e., $f \gg 1$ and hence $A \approx 1$ despite the fact that we have a highly swollen system. ϕ_0 was calculated from the initial molar concentration of monomers, applying the appropriate correction for the sol fraction. (The molar volume of a PNIPA repeat unit is $\bar{V}_{NIPA}$ = 101.5 mL/mol.[11,22])

It is shown below by static light scattering that the weight-average molecular weight of the clay particles, $M_{w,clay}$, corresponds to $\sim 1.7 \times 10^6$ g/mol. With that, an average value of the effective functionality of the clay particles, f_{eff}, can be calculated by

$$f_{eff} = 2\upsilon_{eff}\phi_0 \frac{M_{w,clay}}{C_{RDS}} \tag{4}$$

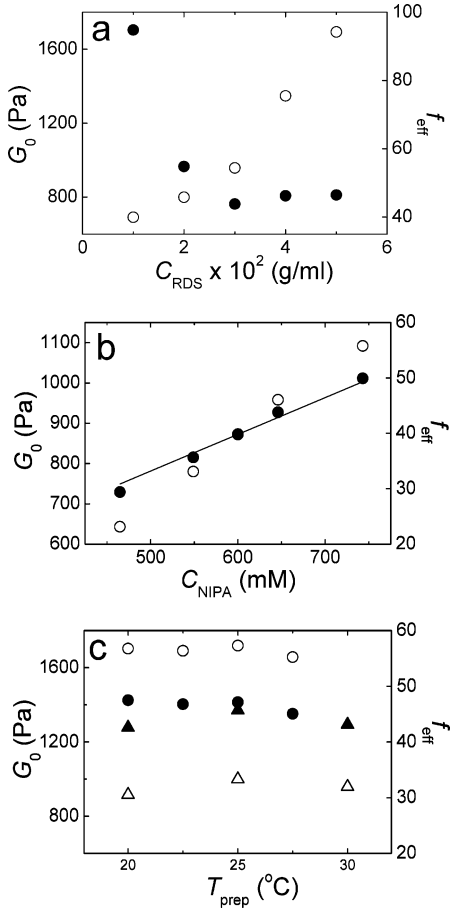

Figure 1. Elastic modulus G_0 (open symbols) and the average effective functionality of clay particles f_{eff} (solid symbols) of nanocomposite hydrogels prepared at different clay concentration, C_{RDS}, monomer concentration, C_{NIPA}, and preparation temperature, T_{prep}. (a) C_{NIPA} = 646 mM, T_{prep} = 25 °C, C_{RDS} = variable. (b) C_{NIPA} = variable, T_{prep} = 25 °C, C_{RDS} = 0.03 g/mL. (c) C_{NIPA} = 646 mM, T_{prep} = variable, C_{RDS} = 0.03 g/mL (triangles) or 0.05 g/mL (circles). The solid line in (b) is a fit of f_{eff} through the origin.

where C_{RDS} is the mass concentration of clay particles at preparation. This means that f_{eff} is given by twice the number of elastically active network chains per clay particle.

On the assumption that the polymer material solely forms effective network chains, the average length of the network chains (number of repeat units between cross-links, N) can be calculated according to

$$N = \frac{1}{\nu_{eff}\bar{V}_{NIPA}} \tag{5}$$

Equation 5 is only correct if there were no elastically ineffective chains. Otherwise, N would be overestimated.

The shear modulus G_0 of the gels measured in the state of sample preparation and the quantities derived from it, viz. ν_{eff}, f_{eff}, and N, are compiled in Table 1 for different preparation conditions.

Figure 1 shows the shear modulus G_0 and the effective functionality of clay particles f_{eff} of three series of gels as a function of preparation temperature (T_{prep}), concentration of clay (C_{RDS}), and monomer (C_{NIPA}). The shear modulus G_0 increases with rising concentration of clay (Figure 1a) or monomer (Figure 1b). This is the same tendency as that generally observed for chemically cross-linked gels.[11] It was also reported for PNIPA or poly(*N*,*N*-dimethylacrylamide) (PDMAA)/Laponite XLG nanocomposite hydrogels.[16,23] Interestingly, the shear modulus of PNIPA/Laponite RDS hydrogels is found to be independent of the preparation temperature in the range covered by our experiments (Figure 1c). This behavior differs from that of chemically cross-linked PNIPA gels prepared by cross-linking copolymerization, where the modulus drops markedly with rising preparation temperature. As the temperature approaches the LCST (around 32 °C),[24,25] the solvent quality decreases leading to less expanded coil sizes of growing chains. Therefore, the probability for intramolecular cross-linking (or cyclization) increases while that for intermolecular cross-linking is diminished. As a result, the cross-linking efficiency in chemically cross-linked PNIPA gels drops with rising temperature. That a similar behavior is not observed with PNIPA gels cross-linked by Laponite RDS particles may be due to the fact that the interaction between clay and polymer also increases with rising temperature, and thus the two effects neutralize one another.

We will now focus our discussion on f_{eff}, the number of elastically effective network chains per clay particle. f_{eff} is far larger than 1 for all of the samples studied, which justifies the assumption of $A \approx 1$ in eq 3. f_{eff} is in the same order of magnitude as that reported by Haraguchi et al. for PNIPA/Laponite XLG and PDMAA/Laponite XLG nanocomposite hydrogels.[16,23] It must be emphasized that the total number of polymer chains bound to one clay particle may be much larger than f_{eff}, since an appreciable fraction of chains may not connect different clay particles and cannot store elastic energy upon deformation of the network.

When the concentration of monomer is fixed, f_{eff} decreases substantially when the clay concentration is raised from 0.01 to 0.03 g/mL (Figure 1a). Upon further increase of the clay content up to 0.05 g/mL, it remains almost constant. On the other hand, f_{eff} is proportional to the concentration of monomer when the concentration of clay is fixed, as shown in Figure 1b (the solid line is a linear fit through the origin). It is intuitive that f_{eff} should be zero when there is no monomer in the solution. When both the concentration of clay and monomer are fixed, f_{eff} is independent of the preparation temperature of the gels (Figure 1c).

The course of f_{eff} observed when one of the three parameters is varied seems reasonable and consistent: With increasing the concentration of clay for a given concentration of monomer, the probability of finding monomers for a clay particle will certainly decrease, leading to a decrease of f_{eff}. Contrarily, with increasing the concentration of monomer for a given concentration of clay, the probability of finding monomers for a clay particle will tend to increase, leading to an increase of f_{eff}.

However, the dependence of f_{eff} on clay concentration observed in our study is different from what Haraguchi et al.[16,23] reported for PNIPA/Laponite XLG and PDMAA/Laponite XLG hydrogels. They found that the number of elastically effective chains per clay particle increased when increasing the clay concentration for a given concentration of monomer. Since the clay content in our systems (using Laponite RDS) and their systems (using Laponite XLG) are similar, this contrary tendency of the number of elastically effective chains per clay particle as a function of clay concentration might be explained by the different surface chemistry of the

clay particles. Laponite RDS is modified with pyrophosphate ions ($P_2O_7^{4-}$) so that both faces and edges of the clay particles are negatively charged when the particles are dispersed in an aqueous solution. There is a repulsive electrostatic interaction between the clay particles which forces them to stay separate even at moderate concentrations. This fact is supported by the results of static light scattering experiments, which indicate that the clay particles are uniformly distributed within the solution (see below). On the contrary, the Laponite XLG particles have negatively charged faces and positively charged edges. As a result, suspensions of Laponite XLG in water (without polymer) form gels when the concentration exceeds 3%. This gelation is due to the buildup of house of cards-like structures. In PNIPA/Laponite XLG hydrogels it may cause an additional contribution to the modulus. On the other hand, it is possible that the chemical modification with pyrophosphate changes the interactions between NIPA and clay particles. We consider this not very likely because the surface area of the edges is small compared to that of the faces, but we cannot exclude that the probability of cross-linking is influenced by small differences in the chemical nature of the clay particles. These issues are rather complicated and need further investigation, which is beyond the scope of the present work.

Swelling Behavior. The PNIPA/Laponite RDS hydrogels exhibit large, but finite, swelling when placed in an excess of water. The equilibrium swelling ratios, q, listed in Table 1 are in the range of 110−150. Since the preparation of the gels took place at a polymer volume fraction of about 0.040−0.070, the relative volume change was 5−10-fold, which is a typical number for slightly cross-linked systems.

The Flory−Rehner theory of swelling can be applied to determine the effective network density or, equivalently, the average number of repeat units between successive cross-links, N_q, from the equilibrium swelling ratio.[20,26] We use the subscript q to distinguish it from the quantity N determined by modulus measurements.

The condition for swelling equilibrium is given as

$$\phi + \ln(1-\phi) + \chi\phi^2 + \left(1 - \frac{2}{f}\right)\nu_{\text{eff}}\bar{V}_s\left(\phi^{1/3}{\phi_0}^{2/3} - \frac{\phi}{2}\right) = 0 \tag{6}$$

The first three terms originate from the free energy of mixing, and the last term on the left side is due to the chain elasticity. $\phi = 1/q$ is the polymer volume fraction at swelling equilibrium, while ϕ_0 is that at preparation of the gels. $\bar{V}_s$ is the molar volume of solvent, and χ is the polymer−solvent interaction parameter. Since the functionality of the clay particles is rather large, $(1 - 2/f) \approx 1$, and $\nu_{\text{eff}}\bar{V}_s$ can be expressed as $\nu_{\text{eff}}\bar{V}_s = \bar{V}_s/(\bar{V}_{\text{NIPA}}N_q) = 1/(5.6N_q)$. Equation 6 then reads

$$\phi + \ln(1-\phi) + \chi\phi^2 + \frac{1}{5.6N_q}\left(\phi^{1/3}{\phi_0}^{2/3} - \frac{\phi}{2}\right) = 0 \tag{6'}$$

The concentration dependence of the χ parameter was taken into account according to

$$\chi = \chi_1 + \phi\chi_2 \tag{7}$$

where

$$\chi_1 = (\Delta H - T\Delta S)/k_B T \tag{8}$$

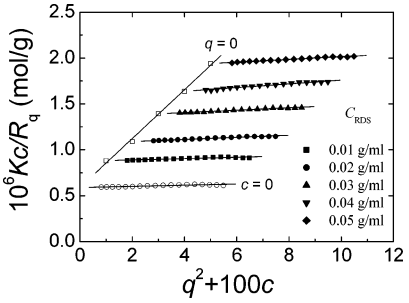

Figure 2. Zimm plot for aqueous suspensions of Laponite RDS. The solid symbols are the experimental data obtained at various clay concentrations, C_{RDS}. The open circles and squares are the extrapolations to zero concentration and zero q, respectively.

The following values determined by Hirotsu were used: $\chi_2 = 0.518$, $\Delta H = -12.462 \times 10^{-21}$ J, and $\Delta S = -4.717 \times 10^{-23}$ J/K.[27]

The quantities N_q thus obtained are also listed in Table 1. Comparison with those obtained by shear modulus measurements shows that the values of N calculated from eq 6′ are in the same range as those obtained by eqs 3 and 5, although in some cases a little smaller. This is similar to the results obtained for PNIPA/Laponite XLG hydrogels.[16] It is not worth discussing this difference in any depth because several reasons can be mentioned which may affect the swelling data and were not taken into account: finite chain extensibility resulting in non-Gaussian behavior, an ionic contribution to the mixing term due to surface charges on the clay particles, etc.[28] It suffices here to state that there is consistency within the limits of the expected precision.

Static Light Scattering. To gain insight into the spatial homogeneity of the hydrogels prepared at different conditions, static light scattering (SLS) experiments were carried out at a constant temperature of 25 °C. In addition to the investigation of the gels, the corresponding systems—aqueous suspensions of clay (without polymer) and solutions of the linear polymer (without clay)—were also studied. It is important to note that the scattering of the gels is markedly stronger than that of systems containing only the clay or only the polymer and also shows a characteristic angular dependence. These facts will be substantiated in the following.

Figure 2 shows a classical Zimm plot of SLS data of the clay suspensions according to the equation

$$\frac{Kc}{R_q} = \frac{1}{M_w}\left(1 + \frac{{R_g}^2q^2}{3} - \ldots\right) + 2A_2c + \ldots \tag{9}$$

where R_q is the Rayleigh ratio of the clay suspension, c is the concentration of the suspension, and K is an optical constant given by

$$K = \frac{4\pi^2n^2(\mathrm{d}n/\mathrm{d}c)^2}{N_A\lambda^4} \tag{10}$$

n is the refractive index of the medium (here $n = 1.331$ for water), and $\mathrm{d}n/\mathrm{d}c = 0.09$ mL/g is the refractive index increment of clay in water at 25 °C.[29] N_A is Avogadro's constant, and λ is the wavelength of the incident light in a vacuum. $q = (4\pi n/\lambda)\sin(\theta/2)$ is the magnitude of the scattering vector with θ being the scattering angle. From the Zimm plot the weight-average molecular

weight of the clay particles, M_w, their radius of gyration, R_g, and the second virial coefficient, A_2, can be determined.

Figure 2 shows that the scattering intensity of clay suspensions with various concentrations in the range 0.01−0.05 g/mL is only slightly dependent on q. The q dependence is similar for all concentrations studied, which indicates that there is no (interparticle) structure in such suspensions in the range of length scales probed by visible light ($2\pi/q$). The slope of the plot of Kc/R_q vs q^2 is thus mainly due to intraparticle interference. From its value extrapolated to zero concentration the radius of gyration R_g is determined to be 18 nm, which is slightly smaller than the value of 23 nm obtained by Nicolai and Cocard.[30] Provided the clay particles form thin circular disks of uniform density, the radius of the disks then is $R = \sqrt{2}R_g = 25$ nm. Recent studies show that Laponite solutions may form a fractal network structure, leading to a power law dependence of the scattering intensity on the scattering vector observed in static light scattering experiments.[31−33] However, Bonn et al.[34] pointed out that the observed "fractal structure" of Laponite solution is most probably due to an incomplete dissolution of clusters of Laponite particles. After careful preparation and filtering the Laponite solution with a 0.8 μm filter, the authors found that there is no structure within the Laponite solution, and the scattering intensity is practically independent of the scattering vector, which is also observed in our experiments as shown in Figure 2.

The molecular weight, M_w, obtained from the simultaneous extrapolation of Kc/R_q to zero concentration and zero scattering angle is 1.7×10^6 g/mol, which is in reasonable agreement with some values reported in literature, viz. $(6.0-6.4) \times 10^5$, 7.1×10^5, 3.0×10^6, and 1.5×10^6 g/mol.[30,35−37]

The second virial coefficient, A_2, obtained from the concentration dependence of Kc/R_q extrapolated to zero q is 1.33×10^{-5} mol·cm^3/g^2. This is well within the usual range found e.g. for flexible polymers in various solvents.[38] When converted into the alternative definition used in ref 35, one obtains $A_2^* = 6.4 \times 10^{-23}$ m^3, which is practically identical to what was reported there. At the highest concentration (0.05 g/mL) used in our experiments, $A_2 \times c \approx 1/M_w$. This means that up to this concentration interparticle interactions are of minor importance. From the obtained molecular weight, M_w, and the radius of the disks, R, the overlap concentration of the clay solution, c^*, can be estimated to be

$$c^* = \left(\frac{M_w}{N_A}\right)\Big/\left(\frac{4\pi}{3}R^3\right) = 0.04 \text{ g/mL} \qquad (11)$$

This is in the range of the highest concentrations used in our experiments. It has to be noted, however, that this estimate is based on the volume of spheres having the same radius as the Laponite disks.

All these different aspects considered support the view that suspensions of Laponite RDS in water at concentrations up to 0.05 g/mL form a random distribution of disklike particles with no perceptible superstructure.

In Figure 3, the scattering curve of a gel made with 0.05 g/mL Laponite RDS and 646 mM NIPA is compared with that of a corresponding suspension of clay (without polymer) and that of a solution of linear PNIPA. Clearly, the scattering intensity of the nanocomposite hydrogel

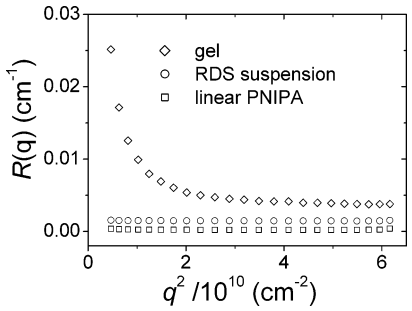

Figure 3. Rayleigh ratio $R(q)$ vs q^2 of a nanocomposite hydrogel with 0.05 g/mL Laponite RDS and 646 mM NIPA as well as the corresponding RDS suspension and linear PNIPA solution.

is significantly higher than that of either of the corresponding systems. Furthermore, the scattering intensity of the gel shows a marked angular dependence with a strong upturn in the lower q range. This situation is typical for all PNIPA/clay nanocomposite hydrogels considered in this paper. The shapes of the scattering curves of the gels differ distinctly from those of chemically cross-linked PNIPA hydrogels, which do not show the strong upturn. This may indicate the presence of large structures as reported by Hecht et al. in polyfluorosilicone (PFSi)/acetone gels.[39]

Generally, the scattering intensity of a gel, $R_{gel}(q)$, is assumed to be due to the sum of thermal concentration fluctuations (ergodic contribution) and of static spatial inhomogeneities resulting from the cross-linking process (nonergodic contribution). The latter is of interest to characterize the microstructure of gels. In an experimental approach to determine this quantity, one presumes that the thermal fluctuations in a gel are practically identical to those in a solution of the linear polymer; hence

$$R_{gel}(q) = R_{sol}(q) + R_{ex}(q) \qquad (12)$$

When the excess scattering, $R_{ex}(q)$, is to be determined for the present experiments, it is not quite clear how to take the scattering of the suspended clay particles into account. One approach would be to subtract from the Rayleigh ratio of the gels not only that of the solution of the linear polymer but also that of the clay dispersion. On the other hand, one might argue that the thermal fluctuations of the clay particles are drastically reduced when they are tied to a fairly large number of polymer chains. According to this second view, the scattering of the clay suspension should not be taken into account. The difference between the two approaches is essentially a shift of the baseline. Since the scattering of the gel exceeds by far the sum of the scattering of both solutions, in particular in the low q range, the difference is of minor importance. We decided to proceed in accordance with the first choice: the excess scattering of the gels was determined by measuring the total scattering of the gel and subtracting the scattering of an un-cross-linked sample of the same polymer concentration plus the scattering of a clay suspension with corresponding concentration.

Figure 4a−c shows the excess scattering of PNIPA/clay nanocomposite hydrogels prepared under different conditions. $R_{ex}(q)$ increases with rising clay concentration (Figure 4a) and with decreasing monomer concentration (Figure 4b). Furthermore, there is a strong dependence on preparation temperature (Figure 4c):

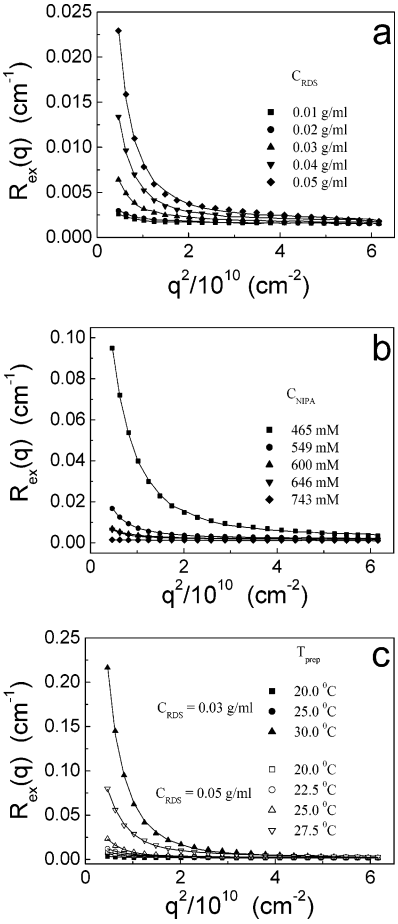

Figure 4. Excess Rayleigh ratio $R_{ex}(q)$ vs q^2 of PNIPA/clay nanocomposite hydrogels prepared at different clay concentration, C_{RDS} (a), monomer concentration, C_{NIPA} (b), and preparation temperatures, T_{prep} (c), with C_{RDS} = 0.03 g/mL (solid symbols) and C_{RDS} = 0.05 g/mL (open symbols). The solid lines are the best fits of eq 13.

The closer the preparation temperature is to the phase transition temperature of PNIPA (LCST ≈ 32 °C), the more heterogeneous is the structure of the gel. These general trends are similar to what was observed with chemically cross-linked PNIPA hydrogels by using *N,N′*-methylenebis(acrylamide) (BIS) as cross-linker.[11] However, there is a fundamental difference between chemically cross-linked gels and gels cross-linked via clay particles with regard to the q dependence of the scattering intensity.

As mentioned above, the dramatic increase of scattering intensity in the lower q range indicates the presence of correlations on a much larger length scale than observed in chemically cross-linked gels. To quantify the correlation lengths, it is necessary to fit the scattering curves according to some model. For a number of networks, the Debye−Bueche approach works reasoably well.[39−42] It was in fact used successfully for the analysis of chemically cross-linked PNIPA hydrogels.[11] However, it is unsuitable to account for the course of the scattering curves of the PNIPA/clay nanocomposite gels. Also, a fit according to the Ornstein−Zernike model[43] did not give reasoable agreement with the experimental data. Plots of log $R_{ex}(q)$ vs log q, which are sometimes used to determine the fractal dimension of heterogeneous systems,[31−33] are markedly nonlinear. Therefore, we get to conclude that our systems may be characterized by several correlation lengths indicating

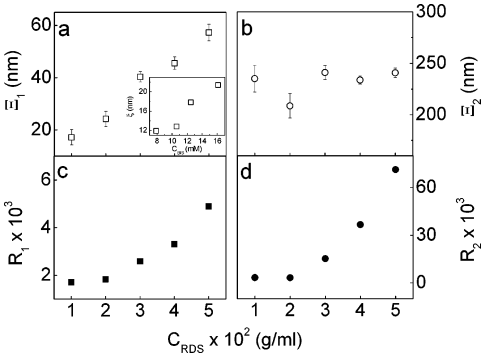

Figure 5. Two correlation lengths, Ξ_1 (a) and Ξ_2 (b), as well as the two prefactors, R_1 (c) and R_2 (d), in PNIPA/clay nanocomposite hydrogels determined with eq 13 as a function of the concentration of clay, C_{RDS}. The inset of (a) is adapted from ref 11, which shows the correlation length ξ of chemically cross-linked PNIPA hydrogels with BIS as cross-linker determined by the Debye−Bueche method.

different levels of organization. Such different types of inhomogeneity or structure can formally be expressed as the sum of given expressions of the scattering intensity. For example, Hecht et al.[39] showed that two Debye−Bueche functions are required to account for the static concentration fluctuations revealed by small-angle neutron scattering in gels based on condensation-cured poly(trifluoropropylmethylsiloxane) in acetone. The same group also reported the existence of two thermodynamic length scales in neutralized polyacrylate gels.[44]

We found that the sum of two exponential functions gives the best fit with our experimental data:[45]

$$R_{ex}(q) = R_1 \exp\left(-\frac{q^2\Xi_1^2}{2}\right) + R_2 \exp\left(-\frac{q^2\Xi_2^2}{2}\right) \quad (13)$$

$$R_j = 4\pi K \Xi_j^3 \langle \eta_j^2 \rangle \quad (14)$$

Here Ξ_j is the jth correlation length, R_j is the corresponding prefactor, and $\langle \eta_j^2 \rangle$ is the jth mean-square fluctuation of refractive index of the gels, with $K = 8\pi^2 n^2 \lambda^{-4}$. The solid lines in Figure 4 are the best fits to eq 13. It is clear that introducing more fit parameters will result in better agreement with experimental data on the expense of the reliability and the physical meaning of these parameters, and particular care is appropriate for the interpretation.

The two static correlation lengths indicate that there are two levels of organization inside the PNIPA/Laponite RDS hydrogels. Note that the scattering intensity of suspensions containing solely clay at various concentrations is almost independent of the scattering angle or scattering vector (cf. Figure 2). This means that the two static correlation lengths are not due to the clay particles themselves, but arise from the interaction between clay particles and PNIPA chains after the formation of the nanocomposite gels.

Figures 5−7 show the obtained correlation lengths, Ξ_1 and Ξ_2, as well as the prefactors of the exponentials, R_1 and R_2, as a function of clay concentration, monomer concentration, and preparation temperature, respectively. Clearly, R_2 is always larger than R_1, in most cases even much larger, indicating that the course of the scattering curves is predominantly determined by the larger correlation length Ξ_2. Ξ_2 is more or less constant in the range 200−250 nm irrespective of how the samples were prepared. This length is appreciably

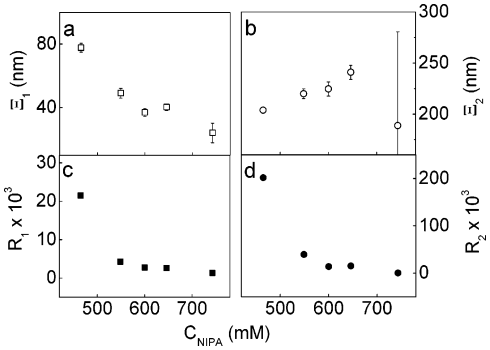

Figure 6. Two correlation lengths, Ξ_1 (a) and Ξ_2 (b), as well as the two prefactors, R_1 (c) and R_2 (d), in PNIPA/clay nanocomposite hydrogels determined with eq 13 as a function of the monomer concentration, C_{NIPA}.

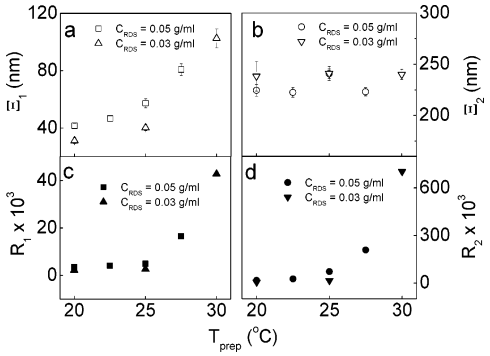

Figure 7. Two correlation lengths, Ξ_1 (a) and Ξ_2 (b), as well as the two prefactors, R_1 (c) and R_2 (d), in PNIPA/clay nanocomposite hydrogels determined with eq 13 as a function of preparation temperature, T_{prep}.

larger than the average spacing of the clay particles (40−65 nm). On the other hand, the smaller correlation length, Ξ_1, is on the same order of magnitude as the correlation length ξ observed in chemically cross-linked PNIPA gels[11] and varies somewhat with preparation conditions.

We shall now discuss the results depicted in Figures 5−7 in more detail. Ξ_1 increases with rising clay concentration (Figure 5a) and decreases with rising NIPA concentration (Figure 6a). These two observations seem to indicate that it is the ratio C_{clay}/C_{NIPA} which is relevant for the characteristic length of the small-scale heterogeneity. The opposite trend is found for the effective number of network chains per clay particle: f_{eff} drops with rising clay concentration and increases with rising NIPA concentration.

The clay particles behave as multifunctional cross-links. This means that they adsorb (or bind) a certain amount of PNIPA, forming brushlike structures with some of the chains connecting different clay particles. Hence, we have an accumulation of polymers in the surroundings of the clay particles. There are regions in between where the PNIPA concentration is lower. It is our understanding that these regions take up only a small fraction of the total volume and thus define the correlation length Ξ_1. When the concentration of PNIPA is raised, the size of the low-concentration regions shrinks and so does Ξ_1. When, on the other hand, the clay concentration is raised, more polymers will accumulate at clay surfaces. This leads to an expansion of the low-concentration regions and an increase of Ξ_1. The consideration of f_{eff} supports this hypothesis. There is still another argument in favor of this view: The correlation volume ω_1, calculated according to $\omega_1 = \Xi_1^3$, is of the order of 10^4-10^5 nm^3. This is appreciably less than the volume available for each clay particle.

From Figure 7a, it is seen that Ξ_1 increases with rising preparation temperature. As solvent quality becomes worse, the PNIPA layers adsorbed at the clay particles assume more compact configurations, leaving more space for the low-concentration regions.

Note that the trend of Ξ_1 with clay concentration, NIPA concentration, and temperature is similar to what was observed previously with chemically cross-linked gels (clay concentration is considered equivalent to concentration of chemical cross-linker), although the numerical values differ somewhat (cf. inset in Figure 5a).[11]

Ξ_2, giving rise to the strong scattering in the low q range and being fairly independent of preparation conditions, corresponds to a correlation volume ω_2 of about 10^7 nm^3. Such a volume comprises about 100−200 clay particles and 3000−5000 active network chains. It is not clear how structural features of this size are generated. They are characteristic of systems cross-linked via nanoparticles and do not occur in chemically cross-linked networks. One might speculate that in the early stages of polymerization there are just a few polymer molecules connecting different clay particles. These molecules impart a stress on the particles trying to pull them closer together. If there were many connecting chains, the stresses acting in different directions would practically cancel out, and the net effect would be to immobilize the particles. However, when there are just a few connecting chains, their local variance is large, resulting in a slightly heterogeneous distribution of the clay particles. Once regions with different density of clay particles have formed, further polymer chains growing in areas of higher particle density are more likely to become connecting chains than those growing in areas of lower particle density. Thus, there is a feedback effect, which finally could be the reason for the large-scale structuring observed.

Figures 5d, 6d, and 7d show that the prefactor R_2, i.e., the extent of large-scale structuring, rises strongly with increasing clay concentration, decreasing concentration of polymer, and rising temperature. Since the redistribution of clay particles is considered the primary cause of the large-scale correlations, the dependence of R_2 on clay concentration is obvious. Lowering the NIPA concentration will tend to enhance the variance of the occurrence of connecting chains, thus leading to stronger large-scale correlations. An increase of temperature means that the solvent gets worse and the polymer chains assume less extended conformations. This effect will also enhance the variance.

According to eq 14, it should be possible to calculate the mean-square fluctuation of refractive index, $\langle \eta_j^2 \rangle$, from R_j and Ξ_j. The exact values of the $\langle \eta_j^2 \rangle$ depend strongly on the precise determination of the corresponding R_j and, in particular, Ξ_j. Since we fitted our scattering curves with four parameters, there is a perceptible uncertainty, and we prefer to confine ourselves here to the above discussion of the prefactors.

Conclusion

The macroscopic properties and spatial inhomogeneities of PNIPA/Laponite RDS nanocomposite hydrogels were systematically investigated by means of mechanical measurements, swelling ratio measurements, and

static light scattering as a function of clay concentration, monomer concentration, and preparation temperature. A striking feature of these gels is the marked angular dependence of scattering intensity showing a strong upturn in the low q range, which sets them apart from chemically cross-linked PNIPA gels. It is interpreted as being due to two levels of organization characterized by two correlation lengths. The smaller correlation length is of the same order of magnitude (several tens of nanometers) as that observed in chemically cross-linked gels. The longer correlation length around 200−250 nm seems to be peculiar to cross-linking via nanoparticles. A corresponding structure is not seen in the aqueous clay suspensions as long as no polymerization of NIPA has occurred. Therefore, we have to conclude that the large-scale structure is built up during the formation of the gels, presumably as a result of a kinetically controlled rearrangement of the clay particles.

The results of measurements of the shear modulus and the equilibrium swelling ratio consistently infer that the clay particles act as multifunctional cross-links with an average effective functionality around 50. It is this high functionality which brings about the large-scale structuring: The network chains are generated in a stepwise manner. When there are just a few at the beginning of gelation, the interconnected clay particles come closer together. The resulting uneven distribution is further enhanced as the reaction progresses and finally leads to the observed scattering features. The enhancement effect can only occur when each particle is able to react repeatedly and is thus characteristic of multifunctional cross-linking species.

Acknowledgment. B. Du thanks the Alexander von Humboldt Foundation for financial support.

References and Notes

(1) Doing, L. C.; Hoffman, A. S. *J. Controlled Release* **1986**, *31*, 7328.
(2) Okano, T. *Adv. Polym. Sci.* **1993**, *110*, 180.
(3) Stayton, P. S.; Shimoboji, T.; Long, C.; Chilkoti, A.; Chen, G.; Harris, J. M.; Hoffman, A. S. *Nature (London)* **1995**, *378*, 472−474.
(4) Stile, R. A.; Burghardt, W. R.; Healy, K. E. *Macromolecules* **1999**, *32*, 7370−7379.
(5) Shibayama, M.; Norisuye, T.; Nomura, S. *Macromolecules* **1996**, *29*, 8746−8750.
(6) Shibayama, M.; Takata, S.; Norisuye, T. *Physica A* **1998**, *249*, 245−252.
(7) Norisuye, T.; Kida, Y.; Masui, N.; Tran-Cong-Miyata, Q.; Maekawa, Y.; Yoshida, M.; Shibayama, M. *Macromolecules* **2003**, *36*, 6202−6212.
(8) Takata, S.; Norisuye, T.; Shibayama, M. *Macromolecules* **2002**, *35*, 4779−4784.
(9) Sayil, C.; Okay, C. *Polym. Bull. (Berlin)* **2000**, *45*, 175−182.
(10) Sayil, C.; Okay, C. *Polymer* **2001**, *42*, 7639−7652.
(11) Nie, J.; Du, B.; Oppermann, W. *Macromolecules* **2004**, *37*, 6558.
(12) Messersmith, P. B.; Znidarsich, F. In *Nanophase and Nanocomposite Materials II*, MRS Symposium Proceedings 457; Komarneni, S., Parker, J. C., Wollenberger, H. J., Eds.; Materials Research Society: Pittsburgh, PA, 1997; p 507.
(13) Xia, X.; Yih, J.; D'Souza, N. A. D.; Hu, Z. *Polymer* **2003**, *44*, 3389−3393.
(14) Liang, L.; Liu, J.; Gong, X. *Langmuir* **2000**, *16*, 9895−9899.
(15) Haraguchi, K.; Takeshita, T. *Adv. Mater.* **2002**, *14*, 1121.
(16) Haraguchi, K.; Takeshita, T.; Fan, S. *Macromolecules* **2002**, *35*, 10162.
(17) Schmidt, D.; Shah, D.; Giannelis, E. P. *Curr. Opin. Solid State Mater. Sci.* **2002**, *6*, 205−212.
(18) Shibayama, M.; Suda, J.; Karino, T.; Okabe, S.; Takehisa, T.; Haraguchi, K. *Macromolecules* **2004**, *37*, 9606.
(19) Oppermann, W.; Rose, S.; Rehage, G. *Br. Polym. J.* **1985**, *17*, 175.
(20) Flory, P. J. *Principles of Polymer Chemistry*; Cornell University Press: Ithaca, NY, 1953.
(21) Treloar, L. R. G. *The Physics of Rubber Elasticity*, 3rd ed.; Clarendon Press: Oxford, 1975.
(22) László, K.; Kosik, K.; Rochas, C.; Geissler, E. *Macromolecules* **2003**, *36*, 7771−7776.
(23) Haraguchi, K.; Farnworth, R.; Ohbayashi, A.; Takeshita, T. *Macromolecules* **2003**, *36*, 5732.
(24) Shild, H. G. *Prog. Polym. Sci.* **1992**, *17*, 163−249.
(25) Wu, C.; Zhou, S. *Macromolecules* **1995**, *28*, 8381−8387.
(26) Flory, P. J.; Rehner, J. *J. Chem. Phys.* **1943**, *11*, 512, 521.
(27) Hirotsu, H. *Adv. Polym. Sci.* **1993**, *110*, 1.
(28) Schröder, U. P.; Oppermann, W. In *The Physical Properties of Polymer Gels*; Cohen Addad, J. P., Ed.; John Wiley: New York, 1996; Chapter 2, pp 19−38.
(29) Avery, R. G.; Ramsay, J. D. F. *J. Colloid Interface Sci.* **1986**, *109*, 448.
(30) Nicolai, T.; Cocard, S. *Langmuir* **2000**, *16*, 8189−8193.
(31) Pignon, F.; Piau, J.; Magnin, A. *Phy. Rev. Lett.* **1997**, *79*, 4689.
(32) Pignon, F.; Piau, J.; Magnin, A. *Phy. Rev. Lett.* **1996**, *76*, 4857.
(33) Mourchid, A.; Levitz, P. *Phys. Rev. E* **1998**, *57*, 4887.
(34) Bonn, D.; Kellay, H.; Tanaka, H.; Wegdam, G.; Meunier, J. *Langmuir* **1999**, *15*, 7534.
(35) Bhatia, S.; Barker, J.; Mourchid, A. *Langmuir* **2003**, *19*, 532−535.
(36) Avery, R. G.; Ramsay, J. D. F. *J. Colloid Interface Sci.* **1986**, *109*, 448.
(37) Rosta, L.; von Gunten, H. R. *J. Colloid Interface Sci.* **1990**, *134*, 397.
(38) Elias, H. G. In *Polymer Handbook,* 4th ed.; Brandrup, J., Immergut, E. H., Grulke, E. A., Abe, A., Bloch, D. R., Eds.; John Wiley & Sons: New York, 1999.
(39) Hecht, A.-M.; Horkay, F.; Geissler, E. *J. Phys. Chem. B* **2001**, *105*, 5637−5642.
(40) Debye, P. J. *J. Chem. Phys.* **1959**, *31*, 680−687. Bueche, F. *J. Colloid Interface* **1970**, *33*, 61. Debye, P.; Bueche, A. M. *J. Appl. Phys.* **1949**, *20*, 518−525.
(41) Soni, V. K.; Stein, R. S. *Macromolecules* **1990**, *23*, 5257−5265.
(42) Kizilay, M. Y.; Okay, O. *Macromolecules* **2003**, *36*, 6856−6862.
(43) Higgins, J. S.; Benoit, H. C. *Polymers and Neutron Scattering*; Clarendon Press: Oxford, 1994.
(44) Horkay, F.; Hecht, A.-M.; Grillo, I.; Basser, P. J.; Geissler, E. *J. Chem. Phys.* **2002**, *117*, 9103−9106.
(45) Geissler, E.; Horkay, F. *Macromolecules* **1991**, *24*, 543−548.

MA050589S